OPEN ACCESS
IOP Publishing
Journal of Physics: Condensed Matter
J. Phys.: Condens. Matter **36** (2024) 325706 (9pp)
https://doi.org/10.1088/1361-648X/ad46d6

Chemical bonding in phase-change chalcogenides

P C Müller[1], S R Elliott[2], R Dronskowski[1] and R O Jones[3,*]

[1] Lehrstuhl für Festkörper- and Quantenchemie, Institut für Anorganische Chemie, RWTH Aachen University, D-52056 Aachen, Germany
[2] Physical and Theoretical Chemistry Laboratory, University of Oxford, Oxford OX1 3QZ, United Kingdom
[3] Peter-Grünberg-Institut PGI-1, Forschungszentrum Jülich, D-52425 Jülich, Germany

E-mail: r.jones@fz-juelich.de

Received 11 February 2024, revised 10 April 2024
Accepted for publication 2 May 2024
Published 17 May 2024

Abstract

Almost all phase-change memory materials (PCM) contain chalcogen atoms, and their chemical bonds have been denoted both as 'electron-deficient' [sometimes referred to as 'metavalent'] and 'electron-rich' ['hypervalent', multicentre]. The latter involve lone-pair electrons. We have performed calculations that can discriminate unambiguously between these two classes of bond and have shown that PCM have electron-rich, 3c–4e ('hypervalent') bonds. Plots of charge transferred between (*ET*) and shared with (*ES*) neighbouring atoms cannot on their own distinguish between 'metavalent' and 'hypervalent' bonds, both of which involve single-electron bonds. PCM do not exhibit 'metavalent' bonding and are not electron-deficient; the bonding is electron-rich of the 'hypervalent' or multicentre type.

Supplementary material for this article is available online

Keywords: chalcogenide materials, chemical bonding, electron-rich multicentre ('hypervalent') bonding, metavalency, phase-change materials, quantum theory of atoms in molecules (QTAIM), density functional calculations

1. Introduction

Phase-change memory materials (PCM) exhibit nanosecond crystallization of amorphous regions in thin polycrystalline layers. The reversible transformations between crystalline and amorphous phases can be initiated by appropriate voltage or laser pulses, and the structural order can be monitored by measuring the electrical resistivity or optical reflectivity. Most PCM are narrow-gap semiconductors having more valence electrons than expected from the Lewis octet rule, which requires that atoms of main-group elements have four pair-bonds. Sb and Te are almost always present, often in alloys near the tie-line $(\mathrm{GeTe})_{1-x}(\mathrm{Sb_2Te_3})_x$ (GST) with metastable, distorted rock salt structures containing cationic vacancies [1].

A recent focus of PCM research has been on the mechanism of bonding in the crystalline state. The results of electronic-structure calculations, for example, have been presented as plots of the number of electrons shared *ES* or transferred *ET* between atoms. These 'maps' have been used to assign particular bonding 'mechanisms' to different families of PCM, assuming that the differences between the properties of crystalline and amorphous PCM are due to a bonding mechanism in the former that is *fundamentally different* from more familiar forms ('covalent', 'metallic', and 'ionic') and therefore warrants a new name, 'metavalent' bonding. These bonds are presumed to involve two-centre, one-electron (2c–1e),

---

[*] Author to whom any correspondence should be addressed.

electron-deficient bonds involving only *p*-electrons, and the materials are referred to as 'incipient metals' [2, 3].

These claims are based on the quantum theory of atoms in molecules (QTAIM) [4], which focuses on the electron density in space-filling, non-overlapping topological domains (atoms) and the electrostatic forces on the nuclei that result. QTAIM calculations can determine *ES* and *ET* for neighbouring domains and have been described as 'precise quantum-chemical descriptors' [2]. 'Maps' like figure 1(a) [2, p 7] have been used to assign labels of different bonding mechanisms, although colour codes are necessary to discriminate between them. In addition to crystalline materials, the authors of [2] included three molecules (ClF_3, XeF_2 and SF_4), where the bonding has been accepted for decades to be electron-rich, with 3c–4e bonds.

In earlier work [5–8] we have shown that the bonding in these chalcogenide materials can be described as multicentre, electron-rich (hypervalent) bonding, and we have emphasized [8] that single-electron bonds are neither 'novel' nor 'fundamentally new'; they have been used successfully in discussing chemical bonding for more than a century to explain the chemical behaviour of molecules that do not satisfy the octet rule [6, 9, and references therein]. These views have been criticized sharply [2, 3][4].

We describe here the results of QTAIM and orbital-based calculations of molecules and crystalline chalcogenide systems, paying particular attention to distinguishing between 'electron-rich' and 'electron-deficient' bonding. In section 2 we discuss points of bonding terminology, and we describe in section 3 the methods of calculation involved and compare the QTAIM and local-orbital results. A discussion (section 4) is followed by our conclusions (section 5).

2. Bonding in PCM

The history of the chemical 'bond' is surveyed in [10], with two distinct classes being 'covalent' and 'ionic' bonds. The balance between kinetic and potential energy in covalent bonding is more subtle than the classical forces present in ionic bonds, and it was many years before the driving force for bond formation was identified as the lowering of the *kinetic* energy due to the *interatomic* delocalization (expansion) of the molecular wave function as atoms come closer [11, 12]. 'Covalency' does not require electron pairing; occupancy of a bonding orbital by a single electron, as in H_2^+, also leads to a 'covalent' bond. Delocalization of the wave function across neighbouring atoms is also essential to describe bonding in metals.

If there are more electrons than needed to satisfy the Lewis octet rule, the molecules are designated as 'electron-rich' or 'hypervalent'. Binding here is usually explained by the three-centre, four-electron (3c–4e) picture [13, 14] with the orbital occupancies shown in figure 2. The presence of formally non-bonding electron pairs ('lone pairs') means that the bond order between adjacent atoms in this bond is 0.5.

Multicentre bonds can also be found in electron-deficient systems—with too few electrons to satisfy the octet rule—and can be understood as 3c–2e bonds [18], also with 'half-bonds' between atoms (figure 2). Such bonds have been been studied for over 70 years [6, and references therein], and single-electron bonds (half-bonds) arise in *both* cases, examples being B_2H_6 (electron-deficient) and XeF_2 (electron-rich). Electron-rich and electron-deficient bonds have similar bond orders and are difficult to distinguish without a multicentre analysis. In 1930, Sugden [9] noted that molecules containing atoms from groups 15–18 of the periodic table could be viewed as covalent compounds that do not violate the octet rule, provided that some of the bonds 'are composed of one shared electron' [9]. Tellurium provides at least half of the atoms in GST compounds, and tellurides dominate the PCM field. The valence configuration of Te ($5s^2 5p^4$) means that the presence of non-bonding electron pairs is inevitable in materials where the Te concentration dominates. The special status of Te is supported by simulations of S, Se, Te, and binary and ternary chalcogenides, which showed significant concentrations of linear 3c–4e bonds in tellurides, but negligible amounts in all crystalline and glassy models of sulphides and selenides [19] (see also [8]).

The nearly-free-electron model of Peierls [20] was applied by Jones [21] in 1934 to the element Bi ($6s^2 6p^3$). He showed that the simple-cubic structure expected for a half-filled *p*-shell distorts to an A7 (rhombohedral) structure, and the weakly broken symmetry and the overlap of conduction and valence bands explain the high diamagnetism and semimetallic conductivity of crystalline Bi. Crucial to these dramatic changes is the presence of five valence electrons in the atom and a stable structure with two atoms per unit cell. For Ge, Sb, and Te, the atomic valence orbitals, as measured by their radial moments, are very similar, and the arguments applied to Bi also explain the rhombohedral structures of GST, which have an average valence (including vacant sites) near five [22].

3. Calculations

3.1. QTAIM and local-orbital calculations

We have performed QTAIM calculations for crystals and for ClF_3, XeF_2, and SF_4, and other small molecules with the programs used in [2] (QUANTUM ESPRESSO [23, 24], CRITIC2 [25]). Densities were calculated using the Bader program [26, 27, and references therein].

The LOBSTER program [16, 17, 28] is also based on density functional calculations, but differs from QTAIM in

---

[4] Wuttig *et al* [2] write: 'These molecules (ClF_3, XeF_2 and SF_4) are located in a very distinct region of the map, remote from other regions, and in particular far away from metavalently bonded chalcogenides. This figure depicts unequivocally that the bonding in electron-rich (3c–4e) molecules has nothing in coming with the bonding mechanism in the chalcogenides discussed here. Hence, … there is no evidence of the participation of four electrons between three centers' [2, p 20] and 'it seems even more misleading to characterize the bonding of GeTe and other crystalline chalcogenides and PCMs (phase change materials) as hypervalent bonding … and … 3c–4e bonding' [2, p 20].

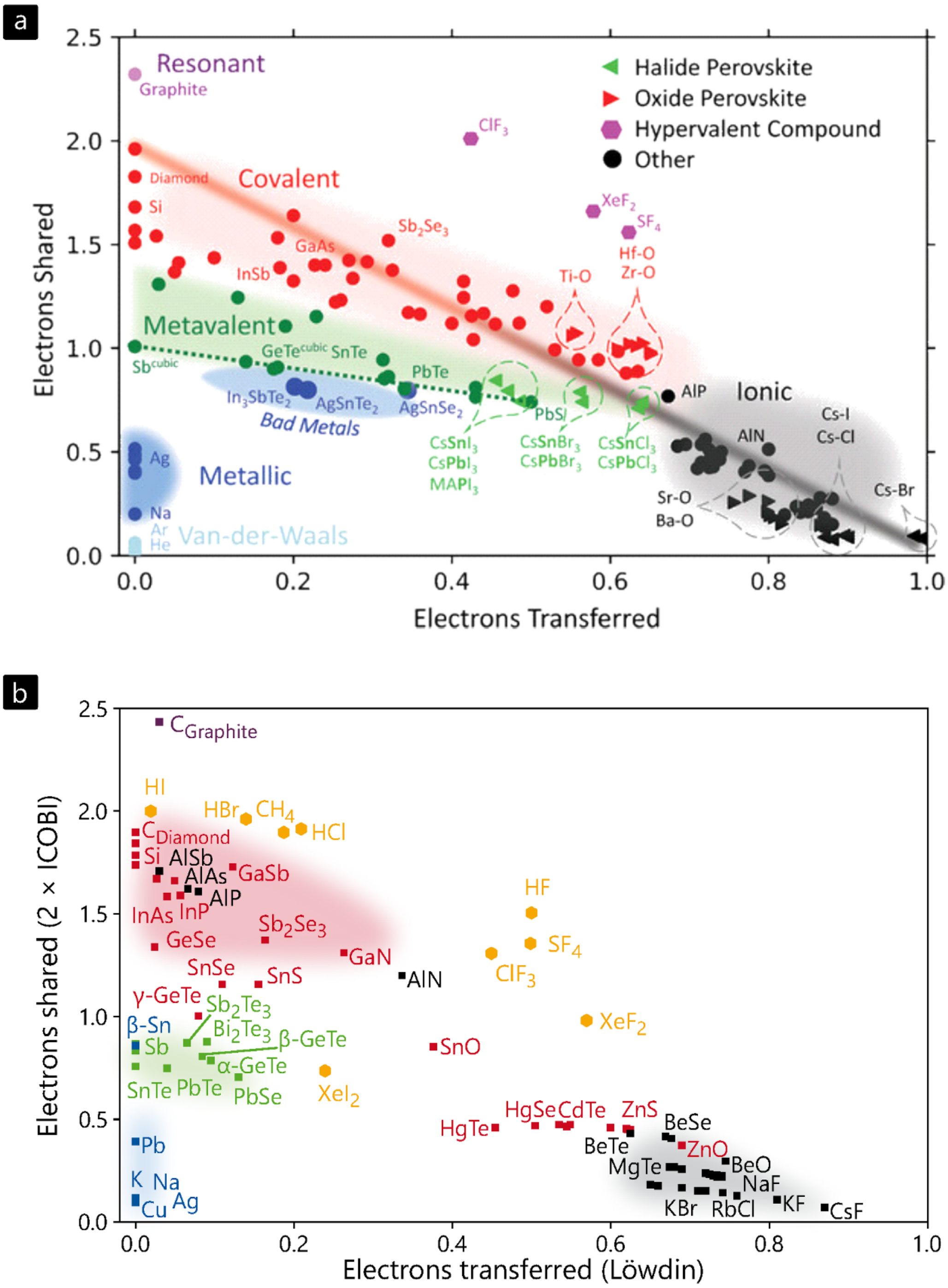

Figure 1. (a) Map classifying chemical bonding in solids, according to [2]. The number of electrons shared between adjacent atomic basins (twice the bond order) is plotted against the electron transfer renormalized by the formal oxidation state (density-based QTAIM calculations) [15]. Different colours aim to characterize different material properties. Hypervalent molecules (3c–4e) are denoted by magenta hexagons. The dashed green line indicates solids with perfect octahedral structures. See also caption of figure 3 in [2]. Adapted from [2] John Wiley & Sons. © 2023 The Authors. Advanced Materials published by Wiley-VCH GmbH. (b) Map showing the average number of electrons shared between adjacent atoms (twice the bond order) plotted against the electron transfer (Löwdin). Hypervalent molecules (3c–4e) are denoted by orange hexagons. Calculations carried out using the LOBSTER program [16, 17].

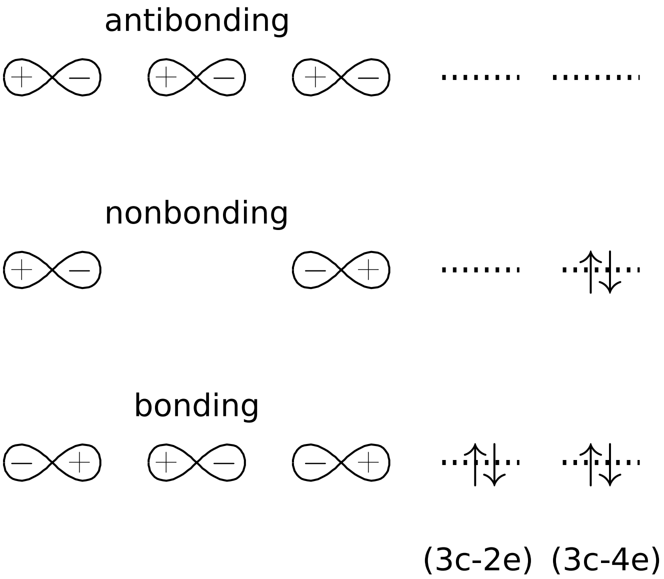

Figure 2. Low-lying molecular orbitals and their occupancies in 3c–2e and 3c–4e 'bonds' in a linear system with p-electrons. Figure 1 in *The chemical bond in solids—revisited* © 2022 by Jones, R O is licensed under CC BY 4.0 [6] https://creativecommons.org/licenses/by/4.0/. Reproduced from [10]. © The Author(s). Published by IOP Publishing Ltd CC BY 4.0.

projecting the Kohn–Sham orbitals (plane-wave basis) onto a local-orbital basis set. Mulliken [29] and Löwdin [30] atomic charges can be calculated, as well as individual and average bond orders (crystal orbital bond indices, COBI) for both molecules and crystal fragments, including those with multicentre bonds. Positive values of the three-centre bond index, for example, imply the presence of a 3c–2e bond, negative values indicate 3c–4e bonding, and a zero value indicates the absence of three-centre bonding [31, 32, and references therein]. This criterion can also be applied to the results of QTAIM calculations [33], and the overlap matrices were extracted here using a modified version of CRITIC2 [25]. In principle, multicentre bonds can also be analyzed using other topological methods [34, and references therein], but these have not yet been applied to PCM.

To compare the QTAIM- and LCAO-based bonding indicators, we calculate the spatial electron densities with both methods. The LCAO-density is accessible from a Mulliken population analysis [29] that can determine the number of electrons $N_{e,\mu}$ in an orbital χ_μ based on the occupation f_j of a molecular orbital (MO) or band j, in terms of the LCAO-coefficients $c_{\mu,j}$ and $c_{\nu,j}$, and their overlap integral $S_{\mu\nu}$:

$$N_{e,\mu} = \sum_j f_j \left(c_{\mu,j}^2 + \sum_{\nu\neq\mu} c_\mu c_\nu S_{\mu\nu} \right) = \sum_j f_j \left(\sum_\nu c_{\mu,j} c_{\nu,j} S_{\mu\nu} \right). \tag{1}$$

For simplicity, the LCAO coefficients and band occupations are replaced by the respective density matrix elements:

$$\begin{aligned}\rho_\mu(\mathbf{r}) &= \sum_j f_j \left(\sum_\nu c_{\mu,j} c_{\nu,j} \chi_\mu(\mathbf{r}) \chi_\nu(\mathbf{r}) \right) \\ &= \sum_\nu P_{\mu,\nu} \chi_\mu(\mathbf{r}) \chi_\nu(\mathbf{r}).\end{aligned} \tag{2}$$

The total electron densities from LCAO and QTAIM are almost identical, so that any differing results will reflect the different partitioning schemes.

MOs are generated by a unitary transformation of a given atomic-orbital basis [35]. In combination with the projection scheme that is implemented in LOBSTER, this method can extract MO from plane-wave calculations, including their mixing coefficients and energy eigenvalues. The definition of a 'molecule' is arbitrary and can be extended to fragments such as Te–Ge–Te and Ge–Te–Ge in crystalline β-GeTe (see below).

3.2. Comparison of QTAIM and local-orbital results

Figure 1(b) plots differences in the Löwdin charges against the average bond order (integrated crystal orbital bond index, ICOBI) for the above molecules and a selection of crystalline materials [15]. The results are very similar to independent calculations of *ES* and *ET* described in [3]. Local-orbital results for ClF_3, XeF_2, and SF_4 are shown in figure 3.

The density-based QTAIM results (figure 1(a)) [2] and the orbital-based (figure 1(b)) analyses show superficial similarities, but important differences:

- QTAIM generally yields larger absolute values of the net charges (Löwdin and Mulliken) than orbital-based population analyses [36, p 155]. The unusually large bond orders found in QTAIM calculations for the ClF_3, XeF_2 and SF_4 molecules (figure 1(a)) are not found in the local-orbital calculations, where the bond orders (figure 3) are much smaller than 1, consistent with multicentre bonds. Large differences in the number of shared electrons *ES* ('covalency') are also found in crystalline materials; the *ES* values of α-GeTe and InSb, for example, differ by 0.15 with QTAIM, and by 0.87 with LOBSTER. QTAIM overestimates *ES* and bond orders for α-GeTe, and the large value of *ES* in ClF_3 (2.14, averaged over (2+1) distinguishable bonds, see figure 3) implies a bond order greater than 1, which is difficult to understand.
- The number of transferred electrons *ET* ('ionicity') are *much* larger in QTAIM calculations than in local-orbital calculations for PCl_3, PCl_5 and other molecules where ionic bonding is significant, as well as for many crystalline materials [37]. AlSb, AlAs, AlP, and AlN are designated 'ionic' in [2], but would be regarded as being 'covalent' with the much smaller *ET* values and ionic charges found in local-orbital calculations. The charge transfer in orbital-based calculations for covalent β-GeTe (rock-salt structure) is just half

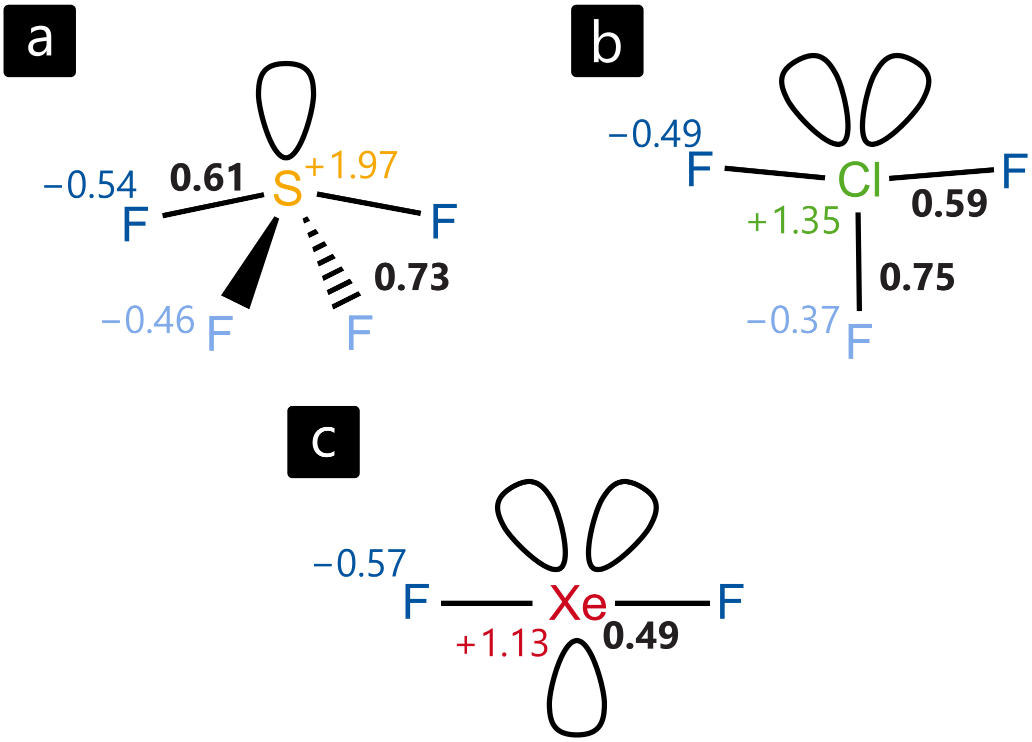

Figure 3. Bond orders (black, bold) and Löwdin charges (corresponding to atomic colours) for molecules with multicentre (hypervalent) bonding: (a) SF_4, (b) ClF_3, and (c) XeF_2 (see figure 1) calculated using the local-orbital method [16, 17].

of the QTAIM value, which is consistent with the negligible difference in electronegativity (0.09, Pauling) between the elements.

- In figure 4, we compare density-based and orbital-based results in more detail for: (a) the multicentre-bonded molecule XeF_2 and (b) crystalline SnTe, both of which have too many electrons to satisfy the octet rule. As noted above, the bond order in the orbital-based calculations is much less than in the QTAIM calculations and corresponds to a single-electron bond; the QTAIM Xe–F bond order (0.92) is much larger than the value (0.5) found in early studies of this molecule [38, 39]. The large electron transfer in the QTAIM calculations for SnTe is also surprising, since the atoms have similar electronegativities. A much smaller transfer is found in the orbital-based calculations.
- The variation of the electron densities along an axis connecting two atoms in these systems is shown in figure 4. The two approaches treat almost identical densities, but the representations are quite distinct. In the QTAIM model, charge originating from *different* atoms is included in domains associated with a specific atom, while in the orbital-related calculations the relationship to the original atoms is maintained.

The bond orders calculated with LOBSTER are 0.46 for B–H in 'electron-deficient' B_2H_6 and 0.49 for Xe–F in XeF_2. The three-centre bond index in B_2H_6 is $+0.39$ [40, pp 170–171]; in XeF_2 it is -0.32 [7], in GeTe -0.099. The bonding in both β-GeTe and molecular XeF_2 is electron-rich, involving non-bonding (lone-pair) orbitals.

Insight into the orbital structure is provided by figure 5, which shows that the frontier orbitals for molecular XeF_2 and fragments of β-GeTe are strikingly similar. XeF_2 is characterized by a p-orbital interaction along the molecular axis, and the shapes of the $2a_{1u}$, $3a_{1g}$, and $3a_{1u}$ states resemble the model of Pimentel and Rundle (figure 2) very closely. A detailed study reveals a contribution of $2s$-orbitals to the a_{1u}-MOs as well as a $5s$-contribution to the a_{1g}-orbital of about 3% and 7%, respectively, based on the squared LCAO coefficients. This agrees with previous findings [41].

The Te–Ge–Te and Ge–Te–Ge fragments in GeTe have the same geometric and electronic properties as the XeF_2 molecule: a linear geometry and an excess of electrons. The MO diagrams of the fragments are also strikingly similar to each other and to the MO of the isolated XeF_2 molecule, with p-orbitals aligned along the three-atom axis and the same ordering. The lowest-lying a_{1u}-orbital is stabilized relative to the atomic energy levels, and the a_{1g}-orbital is close to the p-orbital energies of the outside atoms of the fragments and can be identified as non-bonding. The highest-energy orbital is again of a_{1u} symmetry and shows anti-bonding character. The p-orbitals perpendicular to the axes do not form significant (de-)stabilizing MO, and the s-orbital contributions to the Pimentel–Rundle-style orbitals are of the same order of magnitude as in XeF_2.

Analysis of the QTAIM densities leads to the following three-centre bond indices: β-GeTe (Te–Ge–Te): -0.024; molecular XeF_2 (F–Xe–F): -0.087; molecular B_2H_6:

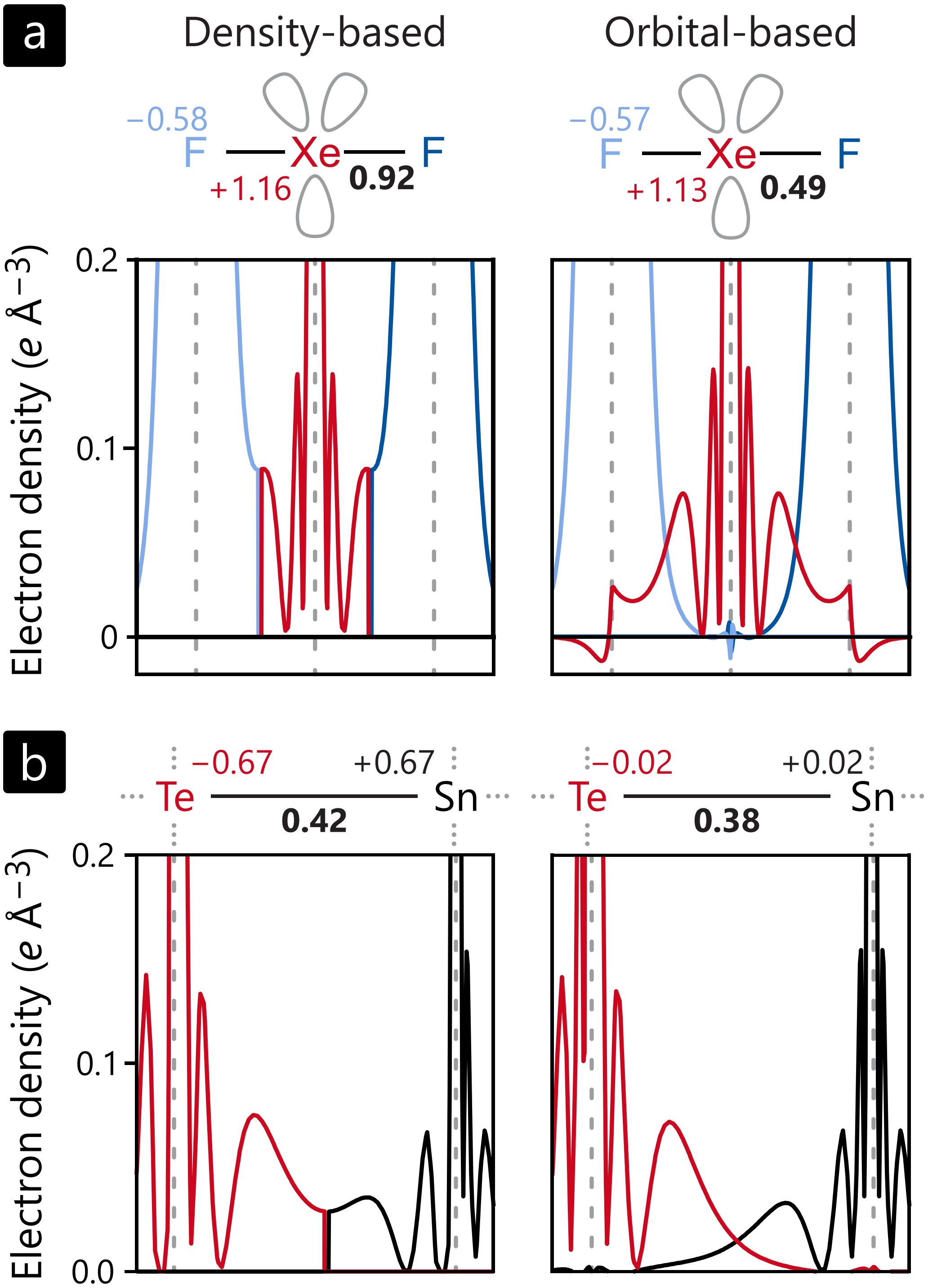

Figure 4. Comparison of density-based and orbital-based results for (a) XeF_2 and (b) crystalline SnTe. The upper part of each frame shows atomic charges and bond orders (black, bold), the lower part the corresponding electron densities along the interatomic axis. The grey vertical dashed lines in the electron-density plots denote the atomic positions.

+0.062. The magnitude of these numbers is smaller than the orbital-based results, but the positive sign in B_2H_6 confirms its status as a classic electron-deficient molecule; the negative signs in the others are consistent with electron-rich bonding. In addition to GeTe (ICOBI(3) value −0.099, see above), we show in figure 6 other materials with compositions $(GeTe)_{1-x}(Sb_2Te_3)_x$, as well as XeF_2 and diamond. All GST crystals have negative three-centred ICOBI: $Ge_3Sb_2Te_6$ ($x = 1/4$, −0.123), $Ge_2Sb_2Te_5$ ($x = 1/3$, −0.130), $GeSb_2Te_4$ ($x = 1/2$, −0.141), Sb_2Te_3 ($x = 1$, −0.153) [7]; all are electron-rich. ICOBI(3) is zero in molecules or crystals that satisfy the octet rule, such as methane CH_4 or diamond. There

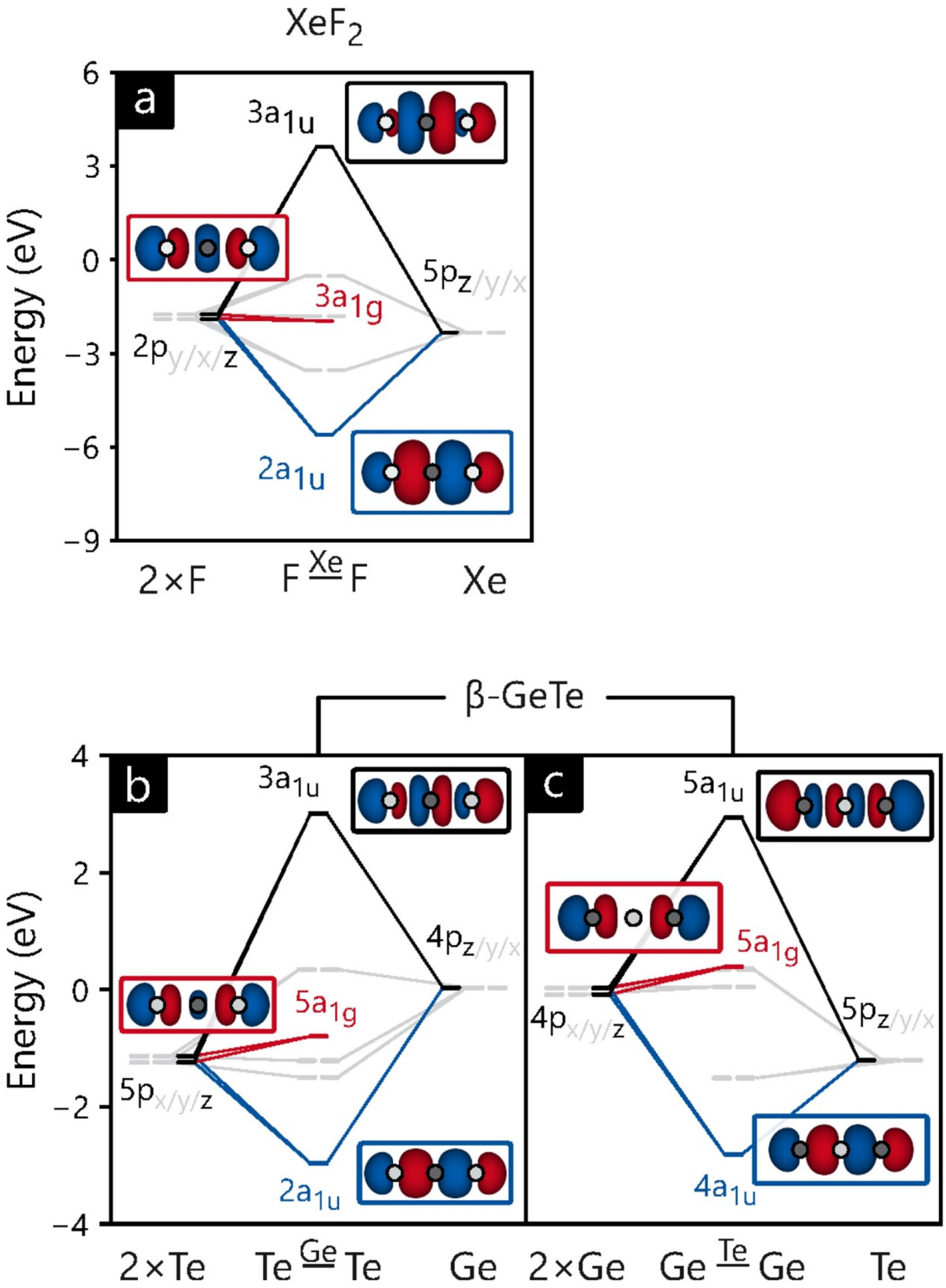

Figure 5. Comparison of the MO diagrams of (a) XeF$_2$, (b) Te–Ge–Te and (c) Ge–Te–Ge in cubic GeTe. The MO corresponding to the 3c–4e bond are shown for all three molecules. Atomic-orbital contributions below 10% are omitted. All energies are relative to the Fermi level. The labelling of the molecular orbitals reflects only the valence electrons of the contributing atoms.

is a linear relationship between ICOBI(3) and the valence electron count (VEC) (figure 6). The fragment orbitals of crystalline, rock salt CaTe, which also satisfies the octet rule, are shown in figure SF1 of the supplementary material [42]. The contrast to the orbitals of GeTe-fragments (figure 5) is clear.

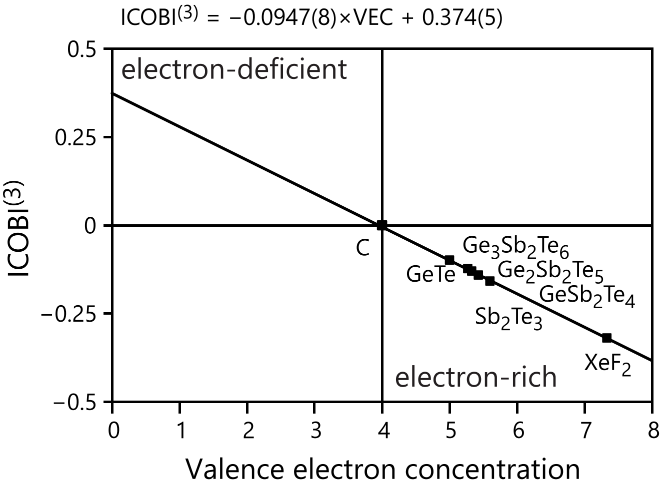

Figure 6. Plot of three-centre integrated crystal order bond index [ICOBI(3)] against average number of *sp*-valence electrons (VEC) in GST phase change materials, diamond, and XeF_2 (local-orbital calculations).

4. Discussion

The proponents of metavalency argue that [2, 3]:

(a) Phase-change materials have unconventional *properties*, including large Born effective charges and Grüneisen parameters, and electrical conductivities between those of metals and insulators. Atom probe tomography (APT) yields *clusters* of atoms, not individual atoms.
(b) This 'unique' property portfolio justifies a separate name ('metavalent') for the bonding mechanism.
(c) Bonds in metavalent materials, e.g. GeTe, PbTe, are two-centre, one-electron bonds (bond order 0.5) involving *p*-electrons. Lone-pair electrons and s-electrons play no significant role. The existence of half-bonds is taken to imply 'electron-deficiency'.
(d) To describe bonds in these materials as being electron-rich ('hypervalent', 3c–4e) bonds is 'unjustified', 'misleading', and 'inadequate', because 'metavalent' solids and 'hypervalent' molecules occupy different regions of plots of the numbers of electrons shared (*ES*) and transferred (*ET*) between adjacent atoms, where *ES* and *ET* are derived from the electron *density* alone. The corresponding plots using orbital-based methods are claimed to be very similar, so that 'concern that the density-based approach is misleading can be refuted' [3].
(e) 'Metavalent' solids are located in these plots between metals (characterized by electron delocalization) and covalent solids (characterized by electron-pair localization, 2c–2e). Their properties are distinctly different from both, and they are termed 'incipient metals'.
(f) *ES* and *ET* can be used to *predict* material characteristics and to tailor properties of chalcogenides.

The properties of PCM [claim (a)] are unusual, but one of the most striking—that *clusters*, not individual atoms, are released from APT—strongly suggests *multicentre* bonding. This is also shown by projected force constants that are only seen for electron-rich materials [43]. Different physical properties do *not* imply different bonding mechanisms [claim (b)] (see below), in particular because the authors of [2] insist that bonding in 'metavalent' chalcogenides, including GeTe, is electron-deficient [claim(c)], without providing a multicentre or other analysis to support this assertion. We have seen, however, that the bonding in GeTe is electron-rich. It is also claimed that the bond order in 'molecules with 3c–4e bonding such as XeF_2 (is) much larger than 1/2' [2, p 20], without providing a published reference.

All 'hypervalent' molecules shown in figure 1(a) [2] are fluorides. Fluorine is the most electronegative element, and significant electron transfer can be expected. Our local-orbital calculations on the hypothetical molecule XeI_2 give *ET* and *ES* values of 0.20 and 0.73, respectively, placing this *hypervalent* molecule very close to the 'metavalent' region. This is a case where 3c–4e bonding is accompanied by little charge transfer. These large uncertainties raise serious doubts about the value of (*ES*,*ET*) maps as property predictors [claim (f)].

The effect of electronegativity is also evident with the halides of hydrogen, where the orbital-based *ET* values are: HF (0.50), HCl (0.21), HBr (0.14), and HI (0.02). These molecules are acidic gases with similar properties, indicating that widely differing *ET* values do not constitute a 'property predictor'. The metals graphite and sodium exhibit 'covalent' and 'metallic' bonding, respectively. On the other hand, similar bonding does not imply similar properties, which is the basis of claims [(d),(e)]. Crystalline diamond and gaseous methane (CH_4) have values of $ES \sim 2$ and $ET = 0$ and 0.18, respectively, both in the covalent region of figure 1(b), while they differ in their most basic property: the state of aggregation.

5. Concluding remarks

We have carried out QTAIM and localized-orbital (LOBSTER) calculations on a range of crystals and molecules. The two approaches lead to significant differences between plots ('maps') of the electron charges shared (*ES*) and transferred (*ET*) between neighbouring atoms. We note that the classification of molecular properties using maps of bond type and structure date back over 90 years [44–46, and references therein]. We have shown unambiguously that 'metavalent' solids and molecules involve multicentre, electron-rich (3c–4e, 'hypervalent') bonds, not two-centre, electron-deficient bonds as claimed by others [2, 3, and references therein].

'Metavalent' bonding is not new. 'Half-bonds' or 'singlet linkages' are long-established feature of both 3c–4e bonds in 'electron-rich' molecules and 3c–2e bonds in 'electron-deficient' molecules, and the presence of half-bonds does *not* imply electron-deficiency. Plots of *ES* and *ET* that are based solely on the density cannot distinguish between electron-rich and electron-deficient bonding. We identify both types of bonds as ‘covalent’—expressed by either constructive orbital interference or kinetic energy lowering—as in metals, where there are fewer electrons per neighbour.

Data availability statement

All data that support the findings of this study are included within the article (and any supplementary files).

Acknowledgments

P C Müller and R Dronskowski gratefully acknowledge financial support from the Deutsche Forschungsgemeinschaft obtained within SFB 917 ‘Nanoswitches.’ S R Elliott gratefully acknowledges the Leverhulme Trust (UK) for a Fellowship and financial support. We thank the Jülich-Aachen Research Alliance (JARA) and the IT Center of RWTH Aachen University for providing computing time (project jara0033).

ORCID iDs

P C Müller https://orcid.org/0000-0001-8329-8030
S R Elliott https://orcid.org/0000-0002-8202-8482
R Dronskowski https://orcid.org/0000-0002-1925-9624
R O Jones https://orcid.org/0000-0003-1167-4812

References

[1] Yamada N 2012 *Phys. Status Solidi* b **249** 1837–42
[2] Wuttig M, Schön C F, Lötfering J, Golub P, Gatti C and Raty J Y 2023 *Adv. Mater.* **35** 2208485
[3] Wuttig M, Schön C F, Kim D, Golub P, Gatti C, Raty J Y, Kooi B J, Martín Pendás A, Arora R and Waghmare U 2024 *Adv. Sci.* **11** 2308578
[4] Bader R F W 1990 *Atoms in Molecules - A Quantum Theory* (Oxford University Press)
[5] Lee T H and Elliott S R 2021 *Phys. Status Solidi* **15** 2000516
[6] Jones R O 2022 *J. Phys.: Condens. Matter* **34** 343001
[7] Hempelmann J, Müller P C, Ertural C and Dronskowski R 2022 *Angew. Chem., Int. Ed.* **61** e202115778
[8] Jones R O, Elliott S R and Dronskowski R 2023 *Adv. Mater.* **35** 2300836
[9] Sugden S 1930 *The Parachor and Valency* (G. Routledge) pp 129–30
[10] Jones R O 2018 *J. Phys.: Condens. Matter* **30** 153001
[11] Ruedenberg K 1962 *Rev. Mod. Phys.* **34** 326–76
[12] Frenking G 2023 *Mol. Phys.* **121** e2110168
[13] Pimentel G C 1951 *J. Chem. Phys.* **19** 446–8
[14] Hach R J and Rundle R E 1951 *J. Am. Chem. Soc.* **73** 4321–4
[15] To simplify comparison of the two maps, we have adopted the convention of [2] in dividing the number of electrons transferred by the formal oxidation state. However, this is not necessary and can lead to unphysical values, e.g. in a system containing a single element with oxidation state of zero or in complex ions where oxidation states cannot be assigned. There are cases where charges carry the opposite sign to the oxidation state, leading to a negative *ET* value
[16] Nelson R, Ertural C, George J, Deringer V L, Hautier G and Dronskowski R 2021 *J. Comput. Chem.* **41** 1931–40
[17] Müller P C, Ertural C, Hempelmann J and Dronskowski R 2021 *J. Phys. Chem.* C **125** 7959–70
[18] Rundle R E 1947 *J. Am. Chem. Soc.* **69** 1327–31
[19] Lee T H and Elliott S R 2022 *Nat. Commun.* **13** 1458
[20] Peierls R 1930 *Ann. Phys.* **396** 121–48
[21] Jones H 1934 *Proc. R. Soc.* A **147** 396–417
[22] Jones R O 2020 *Phys. Rev.* B **101** 024103
[23] Giannozzi P *et al* 2009 *J. Phys.: Condens. Matter* **21** 395502
[24] Giannozzi P *et al* 2017 *J. Phys.: Condens. Matter* **29** 465901
[25] Otero-de-la-Roza A, Johnson E R and Luaña V 2014 *Comput. Phys. Commun.* **185** 1007–18
[26] Yu M and Trinkle D R 2011 *J. Chem. Phys.* **134** 064111
[27] Tang W, Sanville E and Henkelman G 2009 *J. Phys.: Condens. Matter* **21** 084204
[28] Ertural C, Steinberg S and Dronskowski R 2019 *RSC Adv.* **9** 29821–30
[29] Mulliken R S 1955 *J. Chem. Phys.* **23** 1833–40
[30] Löwdin P 1950 *J. Chem. Phys.* **18** 365–75
[31] Ponec R and Mayer I 1997 *J. Phys. Chem.* A **101** 1738–41
[32] Sannigrahi A and Kar T 2000 *J. Mol. Struct.* **496** 1–17
[33] Bochicchio R, Ponec R, Torre A and Lain L 2001 *Theor. Chem. Acc.* **105** 292–8
[34] Silvi B 2002 *J. Molec. Struct.* **614** 3–10
[35] Müller P C, Schmit N, Sann L, Steinberg S and Dronskowski R 2024 *Inorg. Chem.* accepted
[36] Lepetit C, Fau P, Fajerwerg K, Kahn M L and Silvi B 2017 *Coord. Chem. Rev.* **345** 150–81
[37] Raty J Y, Schumacher M, Golub P, Deringer V L, Gatti C and Wuttig M 2019 *Adv. Mater.* **31** 1806280
[38] Rundle R E 1963 *J. Am. Chem. Soc.* **85** 112–3
[39] Coulson C A 1964 *J. Chem. Soc.* 1442–54
[40] Nelson R, Ertural C, Müller P C and Dronskowski R 2023 Chemical bonding with plane waves *Comprehensive Inorganic Chemistry III* 3rd edn, ed J Reedijk and K Poeppelmeier (Elsevier) pp 141–201
[41] Munzarová M L and Hoffmann R 2002 *J. Am. Chem. Soc.* **124** 4787–895
[42] Supplementary Material shows the frontier orbitals of crystalline (rock salt) CaTe. It is available online
[43] Hempelmann J, Müller P C, Konze P M, Stoffel R P, Steinberg S and Dronskowski R 2021 *Adv. Mater.* **33** 2100163
[44] Grimm H G 1928 *Z. Elektrochem.* **34** 430–7
[45] Fernelius W C and Robey R F 1935 *J. Chem. Ed.* **12** 53–68
[46] Jensen W B 1998 *J. Chem. Ed.* **75** 817–28